Bound States and Scattering Resonances Induced by Spatially Modulated Interactions

Ran Qi and Hui Zhai

Institute for Advanced Study, Tsinghua University, Beijing, 100084, China

We study the two-body problem with a spatially modulated interaction potential using a two-channel model, in which the interchannel coupling is provided by an optical standing wave and its strength modulates periodically in space. As the modulation amplitudes increase, there will appear a sequence of bound states. Part of them will cause a divergence of the effective scattering length, defined through the phase shift in the asymptotic behavior of scattering states. We also discuss how the local scattering length, defined through short-range behavior of scattering states, modulates spatially in different regimes. These results provide a theoretical guideline for a new control technique in the cold atom toolbox, in particular, for alkaline-earth(-like) atoms where the inelastic loss is small.

Feshbach resonances (FR) and optical lattices (OL) are two major techniques in the cold atom toolbox. FR can be used to control the interactions by tuning a bound state in the so-called "closed channel" to the scattering threshold via a magnetic field, laser field, or external confinement [1–4]. At resonance, the *s*-wave scattering length diverges and the system becomes a strongly interacting one. OL can strongly modify the single particle spectrum of atoms, which suppress kinetic energy so that interaction effects are enhanced. With these two methods, many interesting many-body physics phenomena, such as the BEC-BCS crossover, superfluid to Mott insulator transition, and strongly correlated quantum fluids in low dimensions, have been studied extensively in cold atom systems during the last decade [5].

In this Letter we theoretically study a new control tool for cold atom system. It is analogous to OL because it also makes use of two counterpropagating laser fields that lead to a periodic modulation of laser intensity in space; however, its main effect is not manifested on single particle, but on the interaction term when two particles collide with each other. It generates a spatial modulation of two-body interaction, i.e., the two-body interaction potential not only depends on the relative coordinate of two particles under collision, but also depends on their center-of-mass coordinate. As far as we know, this is a situation not encountered in interacting systems studied before, ranging from high-energy and nuclear physics to condensed matter systems. One can expect a spatial modulated interaction potential will result in many fascinating phenomena.

The explicit model under consideration is schematically shown in Fig. 1. The open and closed channels are different orbital states and are coupled by laser field. Such an optical FR has been studied before for uniform laser intensity [2], and has been observed experimentally for both alkaline and alkaline-earth-like Yb atoms [6]. In this Letter we shall consider the situation that the laser field is a standing wave whose intensity, and therefore the coupling strength between open and closed channel, is modulated periodically in space. Such a setup allows one to control spatial modulation of interatomic interaction on the scale of submicron. Recently, this has been realized in ^{174}Yb condensation [7], although the optical standing wave is a pulsed one. Alkaline-earth(-like) atom like Yb is particularly suitable for such an experiment because the narrow $^{1}S_0 - {}^{3}P_1$ intercombination transition line can avoid large inelastic scattering loss. In this experiment, a spatially modulated mean-field energy has been observed from diffraction pattern in a time-of-flight image [7]. However, the theoretical study of this system is still very limited, and even the two-body problem has not been studied. In this work we show that surprises indeed arise even in the two-body problem of this model.

Coupled two-channel model.—We consider a two-body Hamiltonian for a FR in which the open and closed channels are modeled by two square-well potentials [8]

$$\mathcal{H} = -\frac{\hbar^2}{4m}\nabla^2_\mathbf{R} - \frac{\hbar^2}{m}\nabla^2_\mathbf{r} + v(\mathbf{R}, \mathbf{r}), \qquad (1)$$

where $\mathbf{R} = (\mathbf{r_1} + \mathbf{r_2})/2$ and $\mathbf{r} = \mathbf{r_1} - \mathbf{r_2}$. For $r < r_0$,
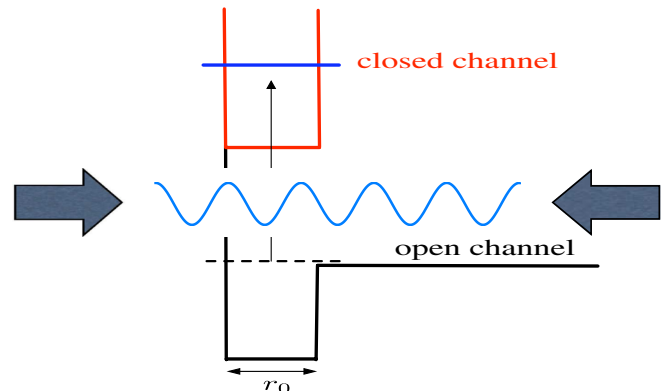

FIG. 1 (color online). A schematic of the model we studied. See text for a detailed description.

$$v(\mathbf{R}, \mathbf{r}) = \begin{pmatrix} -V_o & \hbar\Omega(\mathbf{R}) \\ \hbar\Omega(\mathbf{R}) & -V_c \end{pmatrix} \qquad (2)$$

and for $r > r_0$,

$$v(\mathbf{R}, \mathbf{r}) = \begin{pmatrix} 0 & 0 \\ 0 & +\infty \end{pmatrix}. \qquad (3)$$

In this model V_o is given by the background scattering length a_{bg} as $\tan(k_o r_0)/(k_o r_0) = 1 - a_{\mathrm{bg}}/r_0$ where $k_o = \sqrt{mV_o}/\hbar$, and V_c is determined by the binding energy of closed channel molecule ϵ_c through $V_c = \hbar^2\pi^2/(mr_0^2) - \epsilon_c$. The size of interatomic potential r_0 is much smaller than all the other length scales. Conventionally, the inter-channel coupling $\Omega(\mathbf{R})$ is a constant independent of $\mathbf{R}$. Such a model captures all key features of a FR [4,8]. A bound state appears at threshold and causes scattering resonance at $\Omega_0 = \sqrt{\epsilon_c/|\beta|}$, and the scattering length is given by [8]

$$a_s = a_{\mathrm{bg}}\left(1 - \frac{\beta\Omega^2}{\epsilon_c + \beta\Omega^2}\right), \qquad (4)$$

where $\beta = 32 r_0 a_{\mathrm{bg}}/(9\pi^2)$.

Now consider the situation Ω depends on $\mathbf{R}$. Solving the Schrödinger equation follows two steps. (i) In the regime $r < r_0$, because the $-\hbar^2\nabla_\mathbf{r}^2/m$ term commutes with the Hamiltonian, we consider the wave function of the following form: $\psi_o = \sin(kr)a(\mathbf{R})/r$ and $\psi_c = \sin(kr)b(\mathbf{R})/r$, where $a(\mathbf{R})$ and $b(\mathbf{R})$ satisfy a coupled equation

$$\left[-\frac{\hbar^2}{4m}\nabla_\mathbf{R}^2 - V_o\right]a(\mathbf{R}) + \Omega(\mathbf{R})b(\mathbf{R}) = \epsilon a(\mathbf{R}), \qquad (5)$$

$$\left[-\frac{\hbar^2}{4m}\nabla_\mathbf{R}^2 - V_c\right]b(\mathbf{R}) + \Omega(\mathbf{R})a(\mathbf{R}) = \epsilon b(\mathbf{R}), \qquad (6)$$

where $\epsilon = E - \hbar^2 k^2/m$. There will be a set of eigenfunction $a_l(\mathbf{R})$, $b_l(\mathbf{R})$ and k_l that give rise to the same energy E. The eigenwave function in the regime $r < r_0$ should be assumed as

$$\psi(\mathbf{R}, \mathbf{r}) = \sum_l A_l \frac{\sin k_l r}{r}\begin{pmatrix} a_l(\mathbf{R}) \\ b_l(\mathbf{R}) \end{pmatrix}. \qquad (7)$$

(ii) The superposition coefficient A_l, the binding energy E for bound states, as well as the phase shift $\delta(E)$ for scattering states, are determined by matching the wave function in the regime of $r > r_0$ at $r = r_0$ for any $\mathbf{R}$. The details are shown in the supplemental material [9].

Hereafter we will consider an explicit situation where $\Omega(\mathbf{R}) = \Omega\cos(Kx)$ (x denotes the x component of $\mathbf{R}$). Note that there is still a discrete translation symmetry $x \to x + 2\pi/K$, we can introduce a good quantum number "crystal momentum" q. In the regime $r > r_0$, $\psi_c = 0$, and for the bound states whose energy $E < \hbar^2 q^2/(4m)$, $\psi_o^q(x, r)$ can always be expanded as
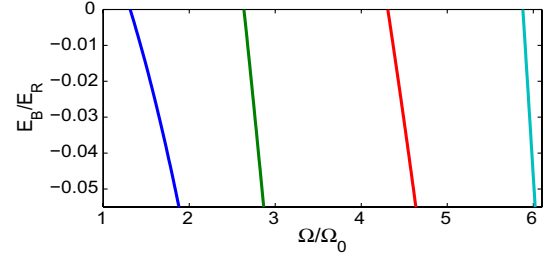

FIG. 2 (color online). First four bound states as a function of the amplitude of coupling Ω/Ω_0. The parameters for this plot are $q = 0$, $\epsilon_c = 0.05 E_R$, $Ka_{\mathrm{bg}} = -0.01$, and $Kr_0 = 10^{-3}$. $E_R = \hbar^2 K^2/m$ is taken as energy unit.

$$\psi_o^q(x, r) = e^{iqx}\sum_n U_n^q e^{inKx}\frac{e^{-r\sqrt{(q+nK)^2 - 4mE/\hbar^2}}}{r}. \qquad (8)$$

Equation (8) can be viewed as the Bloch wave function for molecules. And for the low-energy scattering state whose energy is greater than but close to $\hbar^2 q^2/(4m)$, we have

$$\psi_o^q(x, r) = e^{iqx}\left(U_0^q\frac{\sin(kr - \delta)}{r\sin\delta}\right.$$
$$\left. + \sum_{n\neq 0} U_n^q e^{inKx}\frac{e^{-r\sqrt{(q+nK)^2 - 4mE/\hbar^2}}}{r}\right), \qquad (9)$$

where $k = \sqrt{mE/\hbar^2 - q^2/4}$, and δ is a function of k.

Results 1: bound states.—In contrast to the uniform case where there is only one bound state when $\Omega > \Omega_0$, in this case we find a sequence of bound states as Ω increases, as shown in Fig. 2. This is because the periodic structure of coupling $\Omega(\mathbf{R})$ leads to a "band structure" for the molecules, and as the coupling strength increases, the molecules with zero crystal momentum but in different bands touch the scattering threshold one after the other. We can introduce the "Wannier" wave function as $w(x - x_0, r) = \int_{-K/2}^{K/2} e^{iqx_0}\psi_o^q(x, r)dq$. As shown in Fig. 3, the Wannier function for the bound states that appear at larger Ω have
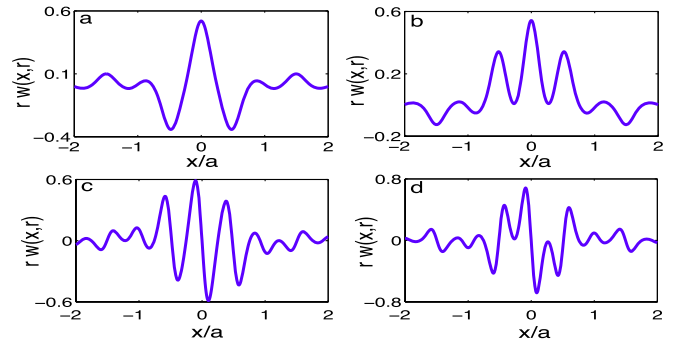

FIG. 3 (color online). $rw(x, r)$ [where $w(x, r)$ is the "Wannier wave function"] for the first four bound states. $a = 2\pi/K$ is the "lattice spacing." The parameters for this plot are $\epsilon_c = 0.05 E_R$, $Ka_{\mathrm{bg}} = -0.01$, $Kr_0 = 10^{-3}$, and $Kr = 0.1$.

TABLE I. Symmetry of Bloch wave function for the first four bound states.

	$U_{-2}^{q=0}$	$U_{-1}^{q=0}$	$U_0^{q=0}$	$U_1^{q=0}$	$U_2^{q=0}$
1st	0	+	0	+	0
2nd	+	0	+	0	+
3rd	+	0	0	0	−
4th	0	+	0	−	0

more oscillation, which means that they come from higher bands. This can also be illustrated from the symmetry of U_n in the Bloch function of Eq. (8), as summarized in the Table I for the first four bound states. The first two bound states have even parity while the other two have odd parity.

Results 2: effective scattering length—For the scattering state wave function, at large **r** only the first term in Eq. (9) will not exponentially decay, and the asymptotic behavior of the scattering wave function is still the same as that in the uniform case. Hence we can introduce an effective scattering length as $a_{\text{eff}} = \lim_{k \to 0} \tan\delta(k)/k$. Note that though the interaction is spatially dependent, the effective scattering length defined above is a spatial independent one. Among the first four bound states, a_{eff} only diverges when the second bound state appears at threshold, as one can see by comparing Fig. 4(a) with Fig. 2. This is because the divergence of a_{eff} implies the first term in Eq. (9) goes like $1/r$, which should be smoothly connected to a zero-energy bound state with nonzero U_0. Therefore, for the other three bound states whose $U_0 = 0$, their couplings to the low-energy scattering states vanish and will not cause divergency of a_{eff}. In Fig. 4(c) we show that a_{eff} diverges when the sixth bound state (whose $U_0 \neq 0$) appears at scattering threshold, but the width of resonance becomes narrower compared to Fig. 4(b) because this bound state comes from higher band and its coupling to low-energy scattering state (i.e., the absolute value of U_0) is smaller.

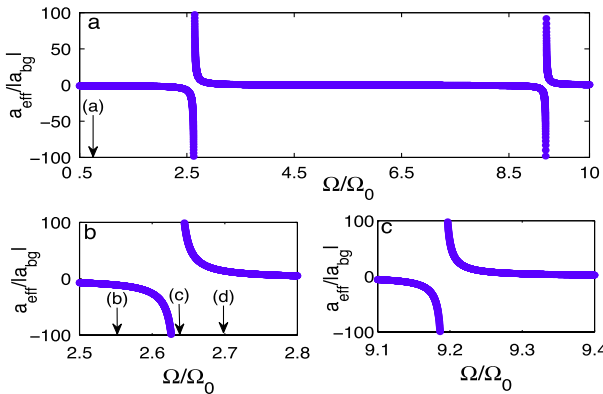*Results 3: local scattering length.*—At short distance the wave function Eq. (9) displays $1/r - 1/a_{\text{loc}}(x)$ behavior, which is consistent with short-range behavior of a contact interaction known as the Bethe-Peierls condition; hence, we can introduce a local scattering length as $a_{\text{loc}}(x) = -\lim_{r \to r_0} \frac{r\psi_o(x,r)}{\partial_r(r\psi_o(x,r))}$. Unlike in the uniform case, a_{eff} and a_{loc} are different. A similar situation has also been encountered for scattering in confined geometry [3], lattices [10], and mixed dimension [11]. What is unique here is that a_{loc} is spatially dependent. Naively, one may think that $a_{\text{loc}}(x)$ can be obtained by replacing Ω in Eq. (4) by local $\Omega(x)$, i.e.,

$$a_{\text{loc}}(x) = a_{\text{bg}}\left(1 - \frac{\beta\Omega^2\cos^2(Kx)}{\epsilon_c + \beta\Omega^2\cos^2(Kx)}\right) \quad (10)$$

$$\approx a_{\text{bg}}[1 - \beta\Omega^2\cos^2(Kx)/\epsilon_c], \quad (11)$$

where the second line is valid for small Ω. This formula in fact corresponds to an oversimplified approximation in our model that the kinetic energy term of the center-of-mass motion $[-\hbar^2\nabla_{\mathbf{R}}^2/(4m)]$ is completely ignored in Eq. (1). In fact, what we really obtained from the wave function Eq. (9) is

$$a_{\text{loc}}(x) = \frac{1 - \sum_{m \neq 0} U_m \cos(mKx)/U_0}{a_{\text{eff}}^{-1} - \sum_{m \neq 0} U_m|m|K\cos(mKx)/(2U_0)}$$

$$\approx \frac{1 - 2U_2\cos(2Kx)/U_0}{a_{\text{eff}}^{-1} - 2U_2 K\cos(2Kx)/U_0}. \quad (12)$$

The second line is also valid when Ω is not too large, so the coefficient $U_{m>2}$ is small enough that it can be ignored.

Away from a resonance, $Ka_{\text{eff}} \ll 1$, Eq. (12) can be well approximated as

$$a_{\text{loc}}(x) = a_{\text{eff}}\left[1 - \frac{2U_2}{U_0}\cos(2Kx)\right]. \quad (13)$$

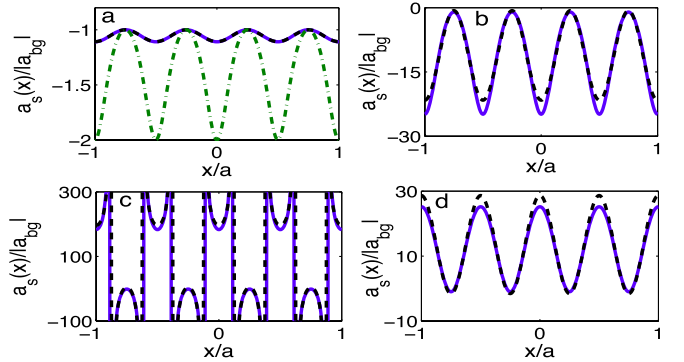In fact, we show in Figs. 5(a), 5(b), and 5(d) that the formula Eq. (13) (dashed black line) is a very good

FIG. 4 (color online). The effective scattering length $a_{\text{eff}}/|a_{\text{bg}}|$ as a function of Ω/Ω_0. (b) and (c) are an enlarged plot around $\Omega/\Omega_0 = 2.64$ (b), 9.20 (c). The arrows indicate the positions at which we plot the local scattering length a_{loc} in Figs. 5(a)–5(d).

FIG. 5 (color online). The local scattering length a_{loc} as a function of position x/a for $\Omega/\Omega_0 = 0.71$, 2.55, 2.64, and 2.7 (a)–(d). The solid blue line is calculated results, the black dashed line is the fitting formula Eq. (13) or (14), and the green dash-dotted line in (a) is from simple replacement formula Eq. (11).

approximation to the actual results (solid blue line). In Fig. 5(a) we show the simple replacement formula Eq. (10) already significantly deviates from the actual results in the weak coupling regime. From Figs. 5(b) and 5(d) one can also see that the mean value of $a_{\mathrm{loc}}(x)$ changes sign as a_{eff} changes sign. At resonance, $a_{\mathrm{eff}}^{-1} \to 0$, Eq. (12) can be approximated as

$$a_{\mathrm{loc}}(x) = \frac{1}{K}\left[1 - \frac{U_0}{2U_2\cos(2Kx)}\right]. \qquad (14)$$

We show in Fig. 5(c) that Eq. (14) is also a very good approximation to actual a_{loc} at resonance. Hence, we show that a_{loc} behaves very differently in the regime near to or away from a scattering resonance.

Implications to many-body physics.—In summary, we have revealed a number of novel features in the two-body problem with a spatially modulated interaction potential, which have strong implications for many-body physics and provide new insights for developing new tools for quantum control in cold atom systems.

First, when a_{eff} diverges, the system enters a strongly interacting regime and is expected to exhibit universal behavior, which can even be manifested in the high-temperature regime [12]. For a two-component Fermi gas, it provides a new route toward BEC-BCS crossover physics, and "high-temperature" superfluid may exist in this regime. The periodic structure will add a new ingredient to crossover physics.

Second, for the low-energy states whose energy $|E| \ll E_{\mathrm{R}}$, the energy dependence of scattering length can be ignored and the many-body system can be effectively described by a pseudopotential model:

$$\hat{H} = -\sum_i \frac{\hbar^2\nabla_{\mathbf{r_i}}^2}{2m} + \sum_{ij}\frac{4\pi\hbar^2 a_{\mathrm{loc}}(\mathbf{R}_{ij})}{m}\delta^3(\mathbf{r_{ij}})\frac{\partial}{\partial r_{ij}}r_{ij}, \quad (15)$$

where $\mathbf{R}_{ij} = (\mathbf{r}_i + \mathbf{r}_j)/2$ and $\mathbf{r}_{ij} = \mathbf{r}_i - \mathbf{r}_j$. It is very important that $a_{\mathrm{loc}}(\mathbf{R})$ in the pseudopotential of Eq. (15) is given by Eq. (12) from the two-body calculation, so that a two-body problem of the Hamiltonian Eq. (15) can produce a correct low-energy eigenwave function and the effective scattering length as from model potential.

For bosons, with a mean-field approximation, Eq. (15) implies that the interaction energy should take the form $E_{\mathrm{mf}} = 4\pi\hbar^2/m \int a_{\mathrm{loc}}(x)n^2(x)dx$, which leads to a modulation of condensate density $n(x)$ and self-trapping nearby the minimum of $a_{\mathrm{loc}}(x)$. It is very likely a strong enough modulation of condensate density will eventually result in the loss of superfluidity and the system will enter an insulating phase. If so, it provides a completely different mechanism for superfluid to insulator transition where the transition is not driven by suppression of kinetic energy as in conventional OL.

Final comments.—In this work we choose a coupled two square-well model whose advantage is that the physics can be demonstrated in a simple and transparent way. However, some more sophisticated effects in the real system, such as inelastic loss, are ignored. We have also implemented more systematic scattering theory which includes these effects and found that the physics discussed here will remain qualitatively unchanged. In particular, the coupling strength required for new resonances is always a few times the strength for conventional optical FR, and therefore is within reach of current experiments. These results will be published elsewhere [13].

Moreover, the formalism used in this work can be easily generalized to other realizations of spatial modulation of interactions. For instance, in a magnetic FR, one can consider the presence of a magnetic field gradient so that the closed channel molecular energy varies spatially. This effect is particularly important for a narrow resonance. One can also optically couple the closed channel molecule to another molecular state via a bound-bound transition, which leads to a periodic variation of molecule energy [14]. Similar effects as discussed in Results 1–3 also present in these cases [13].

[1] E. Tiesinga *et al.*, Phys. Rev. A **46**, R1167 (1992); E. Tiesinga, B. J. Verhaar, and H. T. C. Stoof, Phys. Rev. A **47**, 4114 (1993).

[2] P. O. Fedichev, Yu. Kagan, G. V. Shlyapnikov, and J. T. M. Walraven, Phys. Rev. Lett. **77**, 2913 (1996); J. L. Bohn and P. S. Julienne, Phys. Rev. A **56**, 1486 (1997).

[3] M. Olshanii, Phys. Rev. Lett. **81**, 938 (1998); T. Bergeman, M. G. Moore, and M. Olshanii, Phys. Rev. Lett. **91**, 163201 (2003).

[4] C. Chin, R. Grimm, P. Julienne, and E. Tiesinga, Rev. Mod. Phys. **82**, 1225 (2010).

[5] I. Bloch, J. Dalibard, and W. Zwerger, Rev. Mod. Phys. **80**, 885 (2008).

[6] F. K. Fatemi, K. M. Jones, and P. D. Lett, Phys. Rev. Lett. **85**, 4462 (2000); M. Theis *et al.*, Phys. Rev. Lett. **93**, 123001 (2004); K. Enomoto, K. Kasa, M. Kitagawa, and Y. Takahashi, Phys. Rev. Lett. **101**, 203201 (2008).

[7] R. Yamazaki, S. Taie, S. Sugawa, and Y. Takahashi, Phys. Rev. Lett. **105**, 050405 (2010).

[8] C. Chin, arXiv:cond-mat/0506313.

[9] See supplemental material at http://link.aps.org/supplemental/10.1103/PhysRevLett.106.163201 for details of solving two-body Schrödinger equation.

[10] X. Cui, Y. Wang, and F. Zhou, Phys. Rev. Lett. **104**, 153201 (2010); H. P. Büchler, Phys. Rev. Lett. **104**, 090402 (2010).

[11] Y. Nishida and S. Tan, Phys. Rev. Lett. **101**, 170401 (2008).

[12] T. L. Ho and E. J. Mueller, Phys. Rev. Lett. **92**, 160404 (2004).

[13] R. Qi, P. Zhang, and H. Zhai (to be published).

[14] D. M. Bauer *et al.*, Nature Phys. **5**, 339 (2009).